Using Double-channel and Double-Angle ATSR Data In the Evaluation of Land Surface Temperatures

Jiemin WANG [1] Massimo MENENTI [2]
Akihiko KONDOH [3] Dongqi LIU[1]

[1] Lanzhou Institute of Plateau Atmospheric Physics, Chinese Academy of Sciences, Lanzhou, Gansu 730000, China
[2] DLO Winand Staring Centre for Integrated Land, Soil and Water Research, P.O.Box 125, 6700 AC Wageningen, The Netherlands
[3] Center for Environmental Remote Sensing, Chiba University, Yayoi-cho, Inage-ku, Chiba 263, Japan

Introduction

Land surface temperature (LST) is the most important parameter to be estimated from satellite remote sensing in the study of energy and water budget on land surfaces. There are two major difficulties associated with satellite estimates of land surface temperature: a) the evaluation of atmospheric effects on the measurements from a satellite based sensor; b) the evaluation of emissivity of the land surface. The characteristics of land surface are much more complicated compared with the sea surface. The emissivity of land surfaces varies with landuse type, with vegetation cover and its structure; it may be substantially lower than one, may vary strongly from one point to another, and may have large spectral and angular variation. Consequently, the land surface temperature itself may vary strongly over small distances, within a pixel, leading to difficult average procedure and to some problems in the definition of LST itself.

The split-window method, by using of a linear combination of the radiometric temperatures in channel 4 (11 μm) and channel 5 (12 μm) of the AVHRR, or the similar thermal infrared bands of the Geostationary satellite data, has been fully studied in the estimation of sea surface temperature (SST). Similar simple algorithm was also tried in the estimation of land surface temperature (LST) (Becker and Li, 1990). The task becomes difficult because we still have less knowledge on the variation of the land surface emissivities.

The new ERS-ATSR (Along Track Scanning Radiometer) data consist of 11 μm and 12 μm thermal IR bands (as well as bands at 1.6 and 3.7 μm) and nadir and forward (~54°) measurements, at nearly the same time, which doubles the information as compared with AVHRR. The view geometry for the infrared radiometer of ATSR is shown in Figure 1. One area along the satellite track, with resolution about 1 km for nadir and a little larger for forward, is viewed twice during about two minutes. Assuming the atmosphere is horizontally stratified and stable in this short period, the atmospheric correction should be more accurately determined than by previous methods. Some authors have tried to promote an operational scheme in the estimation of land surface temperatures very recently (e.g. Sobrino et al, 1996).

One set of ATSR data has been used for the algorithm study on deriving surface temperature for a heterogeneous area in Northwest China, where the Heihe River Basin Field Experiment on Land Surface-Atmospheric Interaction (HEIFE, 1990-1993) has been carried out. The experiment region is mainly a large area of Gobi and sand desert with various scales of oasis dispersed along the river and irrigation canals. Surface data

collected during the HEIFE intensive observations, as well as previous studies by using of Landsat TM and NOAA AVHRR are used for the intercomparison. To evaluate the atmospheric effect including atmospheric transmissibility and slant path radiation at the satellite altitude and both of the IR channels of ATSR, the ModTran radiative transfer model has been operated.

Theory & Double-Angle/Double-Channel Technique

Radiance measured on board of the satellite, $B(T_{\lambda\theta})$, as normally expressed,

$$B(T_{\lambda\vartheta}) = \varepsilon_{\lambda\vartheta} B_\lambda(T_s)\tau_{\lambda\vartheta} + R_{atm,\lambda\vartheta\uparrow} + R_{ref,\lambda}\tau_{\lambda\vartheta} \quad (1)$$

Where T is temperature (K), ε is the surface emissivity, τ is the atmospheric transmissibility, the subscript λ denotes the wave band, θ denote the view angle, s denotes the land surface. The second in the right hand of Eq. 1 is the path radiance of the atmosphere, while the third term is the contribution of the surface reflected downward atmospheric radiance. Both terms can be simplified based on minor assumption (Sobrino et al, 1996):

$$R_{atm,\lambda\vartheta\uparrow} = (1-\tau_{\lambda\vartheta})B_\lambda(T_a) \quad (2)$$

$$R_{ref,\lambda} = (1-\varepsilon_{\lambda\vartheta})(1-\tau_{\lambda,53})B_\lambda(T_a) \quad (3)$$

Where T_a is the mean temperature of the atmosphere. For Nadir and Forward of ATSR bands IR3 (10.8μm) & IR4 (12μm), and assuming the transmissibility at 53° is equal to that of forward view, four equations can be Written as following:

$$B(T_{11n}) = \varepsilon_{11n}B(T_s)\tau_{11n} + (1-\tau_{11n})B(T_{a,11n}) + (1-\varepsilon_{11n})(1-\tau_{11f})\tau_{11n}B(T_{a,11n}) \quad (4)$$

$$B(T_{11f}) = \varepsilon_{11f}B(T_s)\tau_{11f} + (1-\tau_{11f})B(T_{a,11f}) + (1-\varepsilon_{11f})(1-\tau_{11f})\tau_{11f}B(T_{a,11f}) \quad (5)$$

$$B(T_{12n}) = \varepsilon_{12n}B(T_s)\tau_{12n} + (1-\tau_{12n})B(T_{a,12n}) + (1-\varepsilon_{12n})(1-\tau_{12f})\tau_{12n}B(T_{a,12n}) \quad (6)$$

$$B(T_{12f}) = \varepsilon_{12f}B(T_s)\tau_{12f} + (1-\tau_{12f})B(T_{a,12f}) + (1-\varepsilon_{12f})(1-\tau_{12f})\tau_{12f}B(T_{a,12f}) \quad (7)$$

The unknowns in the left side of Eq. 4-7, besides the required surface temperature T_s, there are four ε's related to the two wavebands / two view angles (if the atmospheric parameters can be evaluated by observation and transfer models). We must make assumption to reduce the unknowns. Like generally accepted, we first assume that $\varepsilon_{11} = \varepsilon_{12}$, and $\Delta\varepsilon_\theta = \varepsilon_n - \varepsilon_f$.
For easier solution, the separation of T_s and ε is necessary in the above simultaneous equations. Applying the first order Taylor series expansion of the Plank Function B(T), Eq. 4-7 can be rearranged as a function of temperature and emissivity (Sobrino, et al, 1996):

$$T_s = T_{11n} + A_{11}(T_{11n} - T_{11f}) - B_{0,11} + (1-\varepsilon_n)B_{1,11} - \Delta\varepsilon_\vartheta B_{2,11} \quad (8)$$

$$T_s = T_{12n} + A_{12}(T_{12n} - T_{12f}) - B_{0,12} + (1-\varepsilon_n)B_{1,12} - \Delta\varepsilon_\vartheta B_{2,12} \quad (9)$$

Where

$$A_{11} = (1-\tau_{11n})/(\tau_{11n} - \tau_{11f}) \quad (10)$$

$$B_{0,11} = A_{11}(1-\tau_{11f})(T_{a,11n} - T_{a,11f}) \quad (11)$$

$$B_{1,11} = [(1-\tau_{11n}\tau_{11f})/(\tau_{11n}-\tau_{11f})](T_{11n}-T_{11f}) + \tau_{11f}L_{n,11} \quad (12)$$

$$B_{2,11} = \tau_{11f}A_{11}B_{1,11} \quad (13)$$

$$L_{11n} = B(T_{11n})/[\partial B(T)/\partial T]_{T_{11n}} \cong \lambda T_{11n}^2/C_2 \quad (14)$$

There is a similar set of the coefficients for band 12 μm.

Equation 8 and 9 are used for the computation of T_s and ε. However, the unknowns (T_s, ε, and Δε) are still more than the equations. Further estimation of ε by other method is still needed.

The operation of ModTran

The Modtran radiative transfer model was used to calculate the atmospheric transmissibility and radiances for IR3 (11 μm) and IR4 (12 μm) of ERS-1 ATSR at the satellite altitude with the appropriate channel filter functions. The model inputs, particularly the temperature and humidity profiles, are mainly from field measurements at two contrasting stations, one in desert, another in the middle of oasis. The profiles are a composition of following sources:

Surface-1000m: Tethered-balloon sounding
1000-2000m: Low Level Sounding
1000-14000m: Aerological radiosounding
15000m up: Mid-Latitude Summer Model

Total vertical water contents of the atmosphere were calculated to be 1.992 and 1.970 g/cm^2 for oasis and desert respectively. The 'Desert extinction' in the Modtran options is chosen for aerosol attenuation.

The model outputs are summarized in Table 1.

Table 1. Model Outputs for the time when ERS-1 passing (11:30, August 19, 1991)

		11μm		12μm	
		Oasis	Desert	Oasis	Desert
Transmitance	Nadir	0.8632	0.8671	0.7678	0.7728
	Forward	0.7874	0.7933	0.6662	0.6735
Path Radiation W/cm^{2}Sr	Nadir	7.72E-5	7.51E-5	1.27E-4	1.24E-4
	Forward	1.20E-4	1.16E-4	1.86E-4	1.82E-4

The Estimation of Land Surface Emissivity

There were some laboratory and field works on surface emissivity evaluation, but no specific measurements for this during HEIFE. Van de Griend and Owe (1993) proposed a relation between surface emissivity and the satellite sensed vegetation index NDVI, $\varepsilon = 1.009 + 0.047\ln(NDVI)$. We have used it in the regional energy balance study with Landsat TM combined with HEIFE surface observations (Wang et al, 1995). For this study a slightly modified formula is used,

$$\varepsilon = 1.009 + 0.047\ln(NDVI + 0.3) \quad (15)$$

Which seems better particularly for the desert region. On the other hand, Rubio et al (1996)

have investigated large varieties of vegetation, soil and rocks, and postulated a simpler relation for 8-14 μm waveband:

$$\varepsilon_\lambda = a\varepsilon_m + b \tag{16}$$

Where ε_m is the mean effective emissivity for this band, a and b are coefficients given in Table 2 for 11 μm and 12 μm narrow band. In this study, two areas in rather homogeneous part of both desert and oasis in HEIFE region have been chosen respectively, each has 10×10 pixels. Following values are calculated from (16):

Oasis: ε_{11}=0.987 ε_{12}=0.987

Desert: ε_{11}=0.954 ε_{12}=0.971

The values at oasis are similar with that from Eq. 15; while for desert, it is shown here that $\varepsilon_{11} \neq \varepsilon_{12}$. We used a mean value of ε_{11} and ε_{12} in the surface temperature calculations.

Table 2. Mean values and the coefficients of Eq.16 for emissivity calculation in 8-14 μm wavebands by Rubio et al (1997)

	Vegetation			Soil			Rocks		
	a	B	σ	a	b	σ	A	B	σ
11μm	1.619	-0.608	±0.006	0.240	0.742	±0.004	0.231	0.737	±0.02
12μm	1.467	-0.458	±0.009	0.047	0.932	±0.005	0.078	0.898	±0.009
ε_m	0.985±0.002			0.958±0.003			0.936±0.03		

The deficiencies of the ATSR forward view: 'Edge Effect'

The surface resolution for ATSR nadir view is 1 km × 1 km, while that for forward view is 1.5 km × 2 km. The lower resolution of the forward view causes the lower contrast in the T_f images compared with that of T_n, which is clearer for HEIFE area in the boundary of the oasis. Besides, more unrealistic is that if we check the (T_n- T_f) images we found abnormal values at both the north edge and south edge of the oases. At the north edge, when satellite enters over the oasis from the desert, (T_n- T_f) <0. The values of T_f were even 5~8 K lager than T_n at some pixels. Oppositely, at the south edge, when satellite leaves oasis and passes over the Gobi desert, (T_n- T_f)>0, but abnormally large (Figure 2). The normal values are: In the 'training area' of desert, (T_n- T_f) ≈ 0.7 K for 11 μm and 2.4 K for 12 μm; In the training area of oasis, (T_n- T_f) ≈ 3.7 K for 11 μm and 4.0 K for 12 μm. As we know that the surface temperature of desert is about 20 K higher than oasis. The phenomenon mentioned above, called it 'Edge effect' temporally, looks like a kind of delay of response in the ATSR forward view.

To prevent large errors in the surface temperature estimation by using of Eq. 8 and 9, we should pay more attention at the pixels near the edge of the oasis. Some threshold values were set according to following analysis: If we assume

$$(T_n - T_f) = a - b\,T_n \tag{17}$$

Then from the training areas, we have:

Oasis:

11μm $(T_n - T_f) = -211.7278 + 0.7123T_n$

12μm $(T_n - T_f) = -241.6689 + 0.8149T_n$

Desert:

11μm (Tn=310.8) $(T_n - T_f) = -341.1525 + 1.1T_n$

12μm (Tn=314.0) $(T_n - T_f) = -984.4949 + 3.14\,T_n$

An iteration algorithm also used to improve the final estimates.

Results and discussion

The estimated surface temperature of the Heihe River Basin, with method mentioned above, is shown in Figure 3, with a relevant histogram shown in Figure 4. The results have been compared with observations and the previous results from Landsat TM analysis, as shown in Table 3.

Table 3. Comparison of Land Surface Temperatures Observed and Calculated at four HEIFE Stations

Station	*Desert*	*Zhangye*	*AWS013*	*AWS015*
Observation 08/19/1991	44.8	33.4	45.2	47.0
Cal. By Using ATSR	45.0	34.0	50.0	49.0
Observation 07/09/1991	44.8	22.8	17.9	46.5
Cal. By Using Landsat TM	46.5	17.0	16.0	43.7

Concluding Remarks

Using double-channel and double angle IR measurements can improve the evaluation of surface temperature, when compared with the split-window method. This is essential for land surface processes study. To use Eq. 8 and 9, a combination with operation of radiative transfer model is necessary. The evaluation of surface emissivity $\varepsilon(\lambda,\theta)$ is most important in this study. It is necessary to continue the multi-channel (still in the 11~12 μm) multi-view angle space measurements. If the view angle can be add to 3~5, the equations can be solved analytically. For processing ATSR data, the deficiency in the forward view was noticed.

References

Becker, F., and Li, Z., 1990: Towards a local split window method over land surfaces. International Journal of Remote Sensing, 11, 369-394

Rubio, E., V. Caselles, and C. Badenas, 1997: Emissivity measurements of several soils and vegetation types in the 8-14 μm wavebans. Analysis of two field methods. Remote Sensing of Environment, 50, 400-521

Van de Griend, A. A., and M. Owe, 1993: On the relationship between thermal emmisivity and the NDVI for natural surfaces. International Journal of Remote Sensing, 14, 2449-2460.

Wang J., Y. Ma, M. Menenti, W. Bastiaanssen, and Y. Mitsuta, 1995: The scaling-up of processes in the heterogeneous landscape of HEIFE with the aid of satellite remote sensing. Journal of the Meteorological Society of Japan, 73, 6, 1235-1244

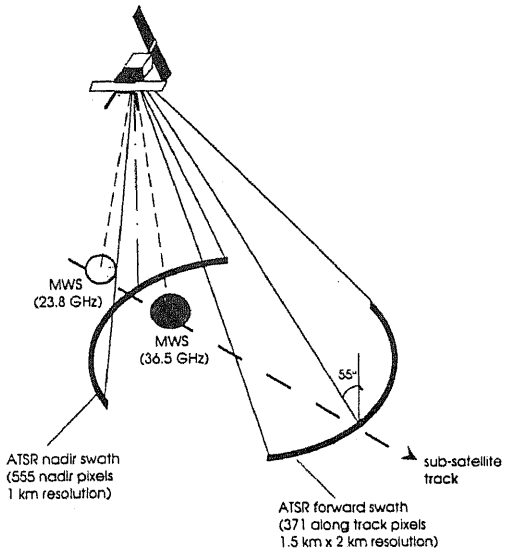

Figure 1. ATSR view geometry

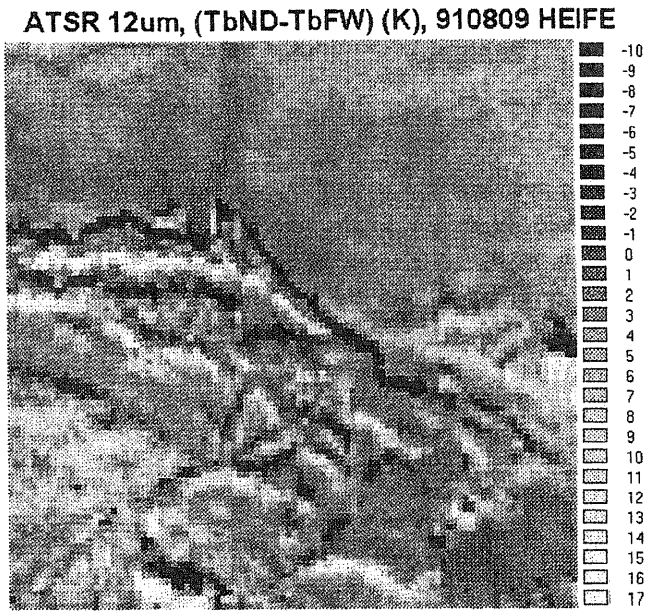

Figure 2. The distribution of brightness temperature difference (T_n-T_f) for 12 μm.

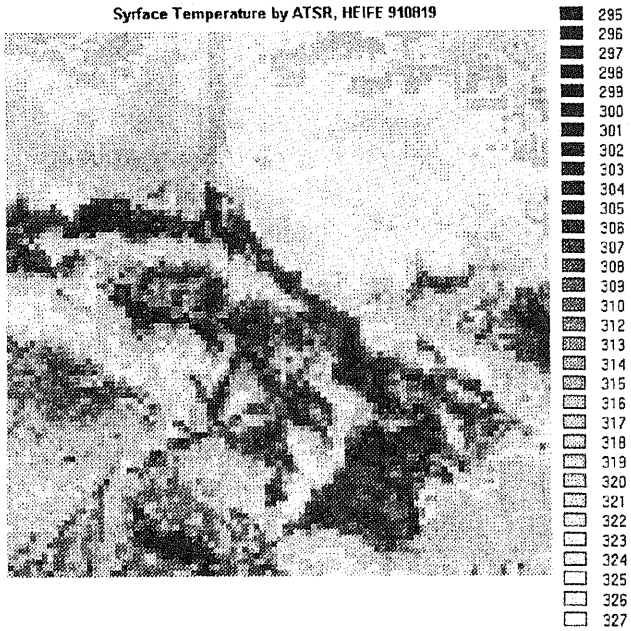

Figure 3. Surface temperature distribution in HEIFE region, calculated by using of ATSR data.

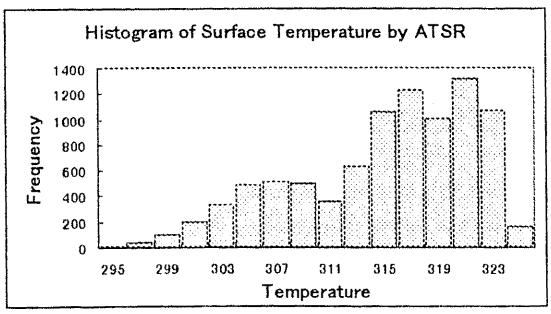

Figure 4. Histogram of surface temperature distribution in Figure 3.